

# H<sup>+</sup>-dependent inorganic phosphate uptake in *Trypanosoma brucei* is influenced by *myo*-inositol transporter

Thais Russo-Abrahão<sup>1,2,3</sup> · Carolina Macedo Koeller<sup>4</sup> · Michael E. Steinmann<sup>5</sup> ·  
Stephanie Silva-Rito<sup>2,3</sup> · Thaissa Marins-Lucena<sup>2,3</sup> · Michele Alves-Bezerra<sup>2,6</sup> ·  
Naira Ligia Lima-Giarola<sup>2,3</sup> · Iron Francisco de-Paula<sup>2,6</sup> · Amaia Gonzalez-Salgado<sup>5</sup> ·  
Erwin Sigel<sup>5</sup> · Peter Bütikofer<sup>5</sup> · Katia Calp Gondim<sup>2,6</sup> · Norton Heise<sup>4</sup> ·  
José Roberto Meyer-Fernandes<sup>2,3</sup>

Received: 1 July 2016 / Accepted: 22 January 2017 / Published online: 9 February 2017  
© Springer Science+Business Media New York 2017

**Abstract** *Trypanosoma brucei* is an extracellular protozoan parasite that causes human African trypanosomiasis or “sleeping sickness”. During the different phases of its life cycle, *T. brucei* depends on exogenous inorganic phosphate (P<sub>i</sub>), but little is known about the transport of P<sub>i</sub> in this organism. In the present study, we showed that the transport of <sup>32</sup>P<sub>i</sub> across the plasma membrane follows Michaelis-Menten kinetics and is modulated by pH variation, with higher activity at acidic pH. Bloodstream forms presented lower P<sub>i</sub> transport in

comparison to procyclic forms, that displayed an apparent K<sub>0.5</sub> = 0.093 ± 0.008 mM. Additionally, FCCP (H<sup>+</sup>-ionophore), valinomycin (K<sup>+</sup>-ionophore) and SCH28080 (H<sup>+</sup>, K<sup>+</sup>-ATPase inhibitor) inhibited the P<sub>i</sub> transport. Gene *Tb11.02.3020*, previously described to encode the parasite H<sup>+</sup>:*myo*-inositol transporter (TbHMIT), was hypothesized to be potentially involved in the H<sup>+</sup>:P<sub>i</sub> cotransport because of its similarity with the Pho84 transporter described in *S. cerevisiae* and other trypanosomatids. Indeed, the RNAi mediated knockdown remarkably reduced *TbHMIT* gene expression, compromised cell growth and decreased P<sub>i</sub> transport by half. In addition, P<sub>i</sub> transport was inhibited when parasites were incubated in the presence of concentrations of *myo*-inositol that are above 300 μM. However, when expressed in *Xenopus laevis* oocytes, two-electrode voltage clamp experiments provided direct electrophysiological evidence that the protein encoded by *TbHMIT* is definitely a *myo*-inositol transporter that may be only marginally affected by the presence of P<sub>i</sub>. These results confirmed the presence of a P<sub>i</sub> carrier in *T. brucei*, similar to the H<sup>+</sup>-dependent inorganic phosphate system described in *S. cerevisiae* and other trypanosomatids. This transport system contributes to the acquisition of P<sub>i</sub> and may be involved in the growth and survival of procyclic forms. In summary, this work presents the first description of a P<sub>i</sub> transport system in *T. brucei*.

**Electronic supplementary material** The online version of this article (doi:10.1007/s10863-017-9695-y) contains supplementary material, which is available to authorized users.

✉ Norton Heise  
nheise@biof.ufrj.br

✉ José Roberto Meyer-Fernandes  
meyer@bioqmed.ufrj.br

<sup>1</sup> Instituto de Microbiologia Professor Paulo de Góes, Centro de Ciências da Saúde, Universidade Federal do Rio de Janeiro, Rio de Janeiro, RJ, Brazil

<sup>2</sup> Instituto de Bioquímica Médica Leopoldo de Meis, Centro de Ciências da Saúde, Universidade Federal do Rio de Janeiro, Rio de Janeiro, RJ 21941-590, Brazil

<sup>3</sup> Instituto Nacional de Ciência e Tecnologia em Biologia Estrutural e Bioimagem, Rio de Janeiro, RJ, Brazil

<sup>4</sup> Instituto de Biofísica Carlos Chagas Filho, Centro de Ciências da Saúde, Universidade Federal do Rio de Janeiro, Rio de Janeiro, RJ 21941-590, Brazil

<sup>5</sup> Institute of Biochemistry and Molecular Medicine, University of Bern, 3012 Bern, Switzerland

<sup>6</sup> Instituto Nacional de Ciência e Tecnologia em Entomologia Molecular, Rio de Janeiro, RJ, Brazil

**Keywords** *Trypanosoma brucei* · P<sub>i</sub> transporter system · Inorganic phosphate

## Abbreviations

AMDP Aminomethylenediphosphonate  
DMSO Dimethyl sulfoxide  
FBS Fetal bovine serum

FCCP	Carbonylcyanide- <i>p</i> -trifluoromethoxyphenylhydrazine
HEPES	4-(2-hydroxyethyl)-1-piperazineethanesulfonic acid
IDP	Imidodiphosphate
PSG	Phosphate-sodium-glucose

## Introduction

African trypanosomiasis is a parasitic disease of medical and veterinary importance affecting mainly the sub-Saharan Africa. Their causative agents, the African trypanosomes, are hemoflagellate and blood-borne unicellular protozoans that are transmitted through the bite of tsetse fly species (*Glossina* spp.) and cause often-fatal diseases in various mammals (Beschlin et al. 2014). Human African trypanosomiasis (HAT) or sleeping sickness is caused by *T. brucei gambiense* and *T. brucei rhodesiense* (Steverding 2008). Animal African trypanosomiasis (AAT) are caused by a large number of species that include *T. congolense*, *T. vivax*, *T. evansi* and *T. brucei brucei* which cause “Nagana” in cattle, and *T. equiperdum* that causes “Dura” in horses (Lopes et al. 2010).

Without prompt diagnosis and treatment, HAT is usually fatal. The parasites multiply in body fluids, cross the blood–brain barrier and invade the central nervous system (WHO 2014). According to Food and Agriculture Organization (FAO), the infection threatens an estimated 60 million people and about 50 million of cattle livestock. AAT causes 3 million deaths in cattle every year and Nagana has a severe impact on agriculture in sub-Saharan Africa (FAO 2015).

It is known that inorganic phosphate ( $P_i$ ) is important for several cellular functions and, in addition, for biochemical reactions related to the transfer of phosphoryl groups (Dick et al. 2014). In *Saccharomyces cerevisiae*, intracellular levels of phosphate are regulated by the *PHO* system. There are two major transporters described: a repressible high-affinity system (active at low concentrations of  $P_i$ ) and a low-affinity system (active at high concentrations of  $P_i$ ). High-affinity system comprises two  $P_i$  transporters, namely Pho84 and Pho89. Pho84 is an  $H^+$ / $P_i$  cotransporter (Persson et al. 1998, 1999), while Pho89 is a  $Na^+$ / $P_i$  cotransporter that is active at alkaline pH (Martinez and Persson 1998). Also in *S. cerevisiae*, the expression of the genes encoding these transporters is regulated by exogenous  $P_i$  concentration through the kinase/cyclin-mediated *PHO* pathway (Auesukaree et al. 2003).  $P_i$  transporters were also described in bacteria, plants and mammalian cells (Harris et al. 2001; Ito et al. 2005; Lamarche et al. 2008; Pavón et al. 2008; Villa-Bellosta and Sorribas 2010). It was reported that Pho84 phosphate permease has the dual function, acting both as transporter and receptor (named “transceptor”). In this case the same phosphate-binding site is involved in both transport and signaling (Kriel et al. 2011; Schothorst et al. 2013).

$P_i$  transporters were recently described in *Plasmodium falciparum*, the causative agent of malaria (Saliba et al. 2006), and several trypanosomatid protozoan parasites, including *T. rangeli*, *Leishmania infantum* and *T. cruzi* (Dick et al. 2012; Russo-Abrahão et al. 2013; Dick et al. 2013). As reviewed previously, *T. rangeli* and *T. cruzi* possesses two independent  $P_i$  incorporation mechanisms:  $Na^+$ -independent  $P_i$  uptake that is most likely  $H^+$ -dependent and  $Na^+$ -dependent  $P_i$  uptake (Dick et al. 2014). In contrast, *L. infantum* possesses only  $H^+$ -dependent  $P_i$  uptake mechanism that is similar to *S. cerevisiae*, wherein  $P_i$  transport and cell growth is modulated by  $P_i$  deprivation (Persson et al. 2003; Vieira et al. 2011; Russo-Abrahão et al. 2013). Regarding the  $P_i$  uptake,  $Na^+$ : $P_i$  and  $H^+$ : $P_i$  transporters probably facilitate the entry of  $P_i$  into the cytosol, which allows  $P_i$  to be utilized by metabolic pathways (Dick et al. 2014). Putative  $P_i$  transporters with high similarity to the yeast Pho84 and Pho89 and the  $Na^+$ : $P_i$  symporter from *P. falciparum* were identified in the genome of several trypanosomatids. Moreover, their corresponding mRNAs were detected in *T. rangeli*, *T. cruzi* and *L. infantum* by qRT-PCR (Dick et al. 2012; Russo-Abrahão et al. 2013; Dick et al. 2013). In *T. brucei*, a putative Pho84 orthologue (Tb11.02.3020), initially annotated in GeneDB/TriTrypDB as a putative sugar transporter, is a  $H^+$ :*myo*-inositol symporter named TbHMIT that is essential for parasite survival in culture (Gonzalez-Salgado et al. 2012, 2015). The  $Na^+$ : $P_i$ -symporter of *P. falciparum* is important for malaria parasites to exploit the  $Na^+$  in the infected erythrocyte cytosol to energize the uptake of solutes (Saliba et al. 2006).

In this work, using biochemical, pharmacological and molecular approaches, we describe for the first time  $P_i$  transport mechanisms in *T. brucei* procyclic forms.

## Materials and methods

### Materials

All reagents were purchased from Merck (Darmstadt, Germany) or Sigma Chemical Co. (St. Louis, MO, USA). Radioactive inorganic phosphate ( $^{32}P_i$ ) was purchased from Instituto de Pesquisas Energéticas e Nucleares (IPEN, Brazil). Distilled water used in the preparation of all solutions was deionized with a Milli-Q system of resins (Millipore Corp., Bedford, MA, USA).

### Cell culture

*Trypanosoma brucei brucei* procyclic forms, strain 427, were grown at 28 °C in SDM-79 medium (LCG Biotechnology, Brazil) supplemented with 10% of foetal bovine serum (FBS) (Vitrocell, Brazil) (de Souza Leite et al. 2007) and the cells were cultured at intervals of 48/72 h. *T. b. brucei* strain with

the plasmid pAG3020 (29–13 procyclic forms co-expressing a tetracycline repressor and T7 polymerase) was cultured at 28 °C in SDM-79 containing 10% FBS, 25 µg/ml hygromycin (Invitrogen, USA), and 15 µg/ml neomycin (G418, Invitrogen, USA) (Gonzalez-Salgado et al. 2012). For experiments, the parasites were harvested from the culture medium by centrifugation at 1500 g, 4 °C for 10 min and washed three times in buffer containing 100 mM sucrose, 20 mM KCl, 5.5 mM glucose and 50 mM Tris (pH 7.2).

The bloodstream form strain 427 was obtained from Dra. Ana Paula Cabral de Araujo Lima from the Instituto de Biofísica Carlos Chagas Filho da UFRJ, and cultivated in HMI-9 medium supplemented with Serum Plus (SAFC Bioscience - USA) at 37 °C in a 5% CO<sub>2</sub> humidified incubator and 10% of FBS. These cells (105) were used to inject into (BALB/c, males, 5–6 weeks) mice following the guidelines approved by the Ethics Committee from Centro de Ciências da Saúde of UFRJ (number IBCCF-085). The bloodstream forms used in the experiments were obtained after 4 days of infection. The parasites were isolated from the blood buffy coat in PSG buffer (3 mM KH<sub>2</sub>PO<sub>4</sub>, 57.2 mM Na<sub>2</sub>HPO<sub>4</sub>, 45 mM NaCl, 5.5 mM glucose at pH 8.0) by DEAE-cellulose chromatography (DE-52, Whatman) as described earlier (Bakker et al. 1999). The cells were washed in PSG buffer and stored on ice (Bakker et al. 1999). For the P<sub>i</sub> transport, the cells were washed in buffer comprising of 116 mM NaCl, 5.4 mM KCl, 55.5 mM glucose and 10 mM HEPES (pH 7.2). Cell numbers were counted using a Neubauer chamber.

### Assay for <sup>32</sup>P<sub>i</sub> transport in *T. b. brucei*

*T. b. brucei* cells (5.0 × 10<sup>7</sup> cells/ml) kept in high (10 mM) or low (1 mM) P<sub>i</sub>, or with different concentrations of *myo*-inositol (Sigma-Aldrich, USA) were incubated at 25 °C for 1 h in a reaction mixture (0.2 ml) containing, unless otherwise specified in the figure legends, 140 mM choline chloride, 1.5 mM CaCl<sub>2</sub>, 5 mM KCl, 10 mM HEPES-Tris (pH 7.2), 1 mM MgCl<sub>2</sub>, 0.1 mM KH<sub>2</sub>PO<sub>4</sub> and 2.5 µCi/nmol <sup>32</sup>P<sub>i</sub> (Dick et al. 2013). For the comparison of bloodstream and procyclic forms, cells were incubated with buffer containing 116 mM NaCl, 5.4 mM KCl, 55.5 mM glucose, 10 mM HEPES (pH 7.2), 0.1 mM KH<sub>2</sub>PO<sub>4</sub> and 2.5 µCi/nmol <sup>32</sup>P<sub>i</sub>. P<sub>i</sub> transport was stopped by adding 0.2 ml of an ice-cold solution containing 140 mM choline chloride, 1.5 mM CaCl<sub>2</sub>, 5 mM KCl, 10 mM HEPES (pH 7.2) and 1 mM MgCl<sub>2</sub>. After washing with the same cold buffer (4 °C), the cells were disrupted by adding 0.1% (w/v) SDS. The mixture containing the <sup>32</sup>P<sub>i</sub> taken up by the cells was then transferred (on a filter paper) to a scintillation vial containing 9.0 ml of scintillation fluid. Blank values of uptake were obtained by exposing the cells to the reaction mixture and keeping them on ice during the time of the experiment (De Koning et al. 2000).

To determine the substrate affinity (K<sub>0.5</sub>) and maximum rate (V<sub>max</sub>) of the P<sub>i</sub> transporter, <sup>32</sup>P<sub>i</sub> uptake was measured at P<sub>i</sub> concentrations over the range 0–0.5 mM. To evaluate the effect of perturbations in the membrane potential of the parasite, we used the H<sup>+</sup> ionophore, FCCP (10 µM). The vacuolar ATPase inhibitor bafilomycin A<sub>1</sub> (100 nM) and the K<sup>+</sup> ionophore valinomycin (100 µM) (Ito et al. 2005; Uyemura et al. 2004; Chintagari et al. 2010) were tested to verify the effect on <sup>32</sup>P<sub>i</sub> transport in *T. brucei*. In addition, we also tested the H<sup>+</sup>, K<sup>+</sup>-ATPase inhibitor, SCH28080 (100 µM), and pyrophosphate analogs, IDP (100 µM) and AMDP (100 µM) (Marchesini and Docampo 2002; Martinez et al. 2002). Control vehicles were water (IDP and AMDP), DMSO 1% (bafilomycin A<sub>1</sub>, valinomycin and SCH28080) and ethanol 1% (FCCP). Uptake values obtained in the presence of the vehicles were similar to the values obtained in water control. P<sub>i</sub> transport was also measured in the absence or presence of *myo*-inositol (10, 300 and 1000 µM). The viability of *T. B. brucei* was verified by MTT (3-(4,5-dimethylthiazol-2-yl)-2,5-diphenyltetrazolium bromide) methodology (Mosmann 1983).

The <sup>32</sup>P<sub>i</sub> in the supernatant of the reaction mixture was identified as the unique radiolabeled molecule by ascending thin layer chromatography on PEI-cellulose sheets. It was used 0.75 M P<sub>i</sub> (pH 3.4) as solvent and the radioactive spots were detected by autoradiography, according to Vieyra et al. 1985.

### Intracellular ATP determination

Intracellular ATP in *T. B. brucei* was measured using an ATP bioluminescence assay kit as described by Martins and colleagues (Martins et al. 2009) with slight modifications. Procyclic forms were incubated with 140 mM choline chloride, 1.5 mM CaCl<sub>2</sub>, 5 mM KCl, 10 mM HEPES-Tris (pH 7.2), 1 mM MgCl<sub>2</sub> and 0.1 mM KH<sub>2</sub>PO<sub>4</sub> and centrifuged at 3000×g. Aliquots of the sedimented parasites (5 × 10<sup>7</sup> cells) were lysed in 0.1 ml of 3% trichloroacetic acid (TCA) supplemented with 2 mM EDTA. Ten minutes later the lysed suspension was centrifuged at 10,000×g for 10 min and clear aliquots (0.02 ml) of the supernatants were added to equal volumes of the luciferin/luciferase buffer. The ATP content was measured in a luminometer (Molecular Devices) as the light emitted at 570 nm within 10 s. A diluted pure ATP solution was used as standard.

### RNA isolation and quantitative PCR (qPCR)

Total RNA was isolated from *T. brucei* procyclics transfected with the plasmid pAG3020 grown in the absence or presence of tetracycline (10 × 10<sup>7</sup> cells) using TRIzol® Reagent (Invitrogen Corporation, Carlsbad, USA) according to the manufacturer's instructions. Total RNA concentrations were determined at 260 nm using a Nanodrop ND-1000 system (Thermo

Scientific, Wilmington, USA), and the RNA samples used had an A260/A280 ratio between 1.8 and 2.0. RNA integrity was checked by native agarose gel electrophoresis. One microgram of RNA was treated with RNase-free DNase I (Fermentas International Inc., Burlington, Canada) and used to synthesize cDNA with a High-Capacity cDNA Reverse Transcription Kit (Applied Biosystems, Foster City, USA). For qPCR, an Applied Biosystems ABI Prism 7500 Real-Time PCR System (Applied Biosystems) and SYBR Green PCR Master Mix (Applied Biosystems) were used under the following conditions: one cycle for 10 min at 95 °C, followed by 50 cycles of 15 s at 95 °C and 45 s at 60 °C. Genes were amplified using the primers (*Tb11.02.3020*–5′-TGGAACAAAGGGGCTCAC-3′ and 5′-TTCAGTGCATTGGGAACCGT-3′; *TcGAPDH* – 5′-GCAGCTCCATCTACGACTCC-3′ and 5′-AGTATCCCCACTCGTTGTCG-3′). Primers were designed using Primer3 software (Rozen and Skaletsky 2000). All assays were performed in duplicates, and GAPDH expression was used for normalization (Giarola et al. 2013). Amplification was followed by melting curve analysis. Moreover, reaction products were subjected to agarose gel electrophoresis to check amplification specificity.

#### ***T. b. brucei* Tb11.02.3020 gene silencing by RNA interference (RNAi)**

The plasmid pAG3020 (Gonzalez-Salgado et al. 2012), containing a fragment of 339 bp spanning nucleotides 842–1181 of the *Tb11.02.3020* gene was used to down-regulate expression by RNAi. *T. B. brucei* procyclic forms 29–13 ( $4 \times 10^7$ ) were isolated from mid-log phase ( $0.5\text{--}0.8 \times 10^7$  cells/ml) by centrifugation at  $1250 \times g$  for 10 min, mixed with 100  $\mu\text{L}$  of electroporation solution of human T cell electroporation kit of Nucleofector (Lonza, USA) containing 15  $\mu\text{g}$  of linearized plasmid pAG3020 with NotI and electroporated with the device U-033 program of AMAXA™ Nucleofector™ (LONZA, USA). Then, the electroporated cells were inoculated in 5 ml of SDM-79 medium containing 15% FBS, 25  $\mu\text{g}/\text{mL}$  hygromycin (Invitrogen, USA), and 15  $\mu\text{g}/\text{mL}$  neomycin (G418, Invitrogen, USA). After 12 h, an aliquot of 3 ml of the culture was diluted  $10\times$  in medium containing 50% of fresh SDM-79 medium and 50% of conditioned SDM-79 medium containing 10% FBS and 2  $\mu\text{g}/\text{mL}$  puromycin (Invitrogen, USA) for the selection of parasites containing the plasmid pAG3020 (SDM-selection). An aliquot of 100  $\mu\text{L}/\text{well}$  were distributed into 96-well plates (Corning, USA) which were sealed with parafilm and kept in a moist chamber at 26 °C. After 10–14 days, puromycin antibiotic resistant clones were diluted in SDM-selection 1:5 and transferred to 24-well plates (Corning, USA). After three cycles of dilution 1:5 to expand the cultures, the parasites were tested for the presence of plasmid pAG3020 by PCR reaction using oligonucleotides pALC14-F (5′-TTCGAGTTTTTTTTTCTTTTCCCC-3′)

and Tb3020R (5′-GCTCTAGACTCGAGTGGGAA CACCTGTGAAACAA-3′). Total DNA was extracted from parasites with *TotalPure DNA* (BioAgency, USA) following the manufacturer's instructions. The PCR reaction was performed in a final volume of 20  $\mu\text{L}$  containing Taq buffer (Biotools, USA), total DNA (10 ng), primers described above at 0.8  $\mu\text{M}$  and 1 U of Taq DNA polymerase (Biotools, USA). The tubes were heated to 94 °C ("hot-start") prior to addition of DNA polymerase. The incubation tubes program was 94 °C (30 s), calculated annealing temperature of 58 °C (45 s) and 72 °C (1 min) of length, with this cycle repeated 29X, followed by a final incubation for 9 min, 72 °C. Control reactions were incubated under the same conditions but in the absence of total DNA template or in the presence of pAG3020 plasmid. For all analyzes, the DNA containing samples were subjected to electrophoresis on agarose gel 1% type LE (Promega, USA) containing ethidium bromide 0.5  $\mu\text{g}/\text{mL}$  (BioAgency, Brazil). The 1 kb *GeneRuler* (Fermentas, USA) was used as the DNA size standard. After electrophoresis, the gels were visualized by UV trans-illuminator and the results of separations photo-documented using *ImageQuant* system (GE Healthcare, USA). The induction of RNAi was started by addition of 1  $\mu\text{g}/\text{mL}$  tetracycline (Sigma, USA) to the parasite cultures.

#### **Expression and functional characterization of Tb11.02.3020 in *Xenopus* oocytes**

The *Tb11.02.3020* gene was amplified using primers Tb3020–2-F (5-CCGCTCGAGATGAAGTGGCCGCGTGAAGAT-3) and Tb3020–2-R (5-CCCAAGCTTCTAAATGGGCGCACGGGC-3), resulting in plasmid pAG3020–2, and inserted between the XhoI and HindIII sites of pCDNA3.1(–) vector (Invitrogen). From the linearized vector, the capped cRNA was synthesized (Ambion, Applied Biosystems, Rotkreuz, Switzerland), and a poly(A) tail of about 300 residues was added to the transcript using yeast poly(A) polymerase (USB, USA). Aliquots containing 100 nM RNA were prepared from this stock solution and stored at  $-80$  °C. *Xenopus laevis* oocytes were prepared, injected, and defolliculated as described previously (Gonzalez-Salgado et al. 2012; González-Salgado et al. 2015). Each oocyte was injected with 50 nl of cRNA solution (5 fmol of RNA/oocyte) followed by incubation in modified Barth's solution (10 mM HEPES, pH 7.5, 88 mM NaCl, 1 mM KCl, 2.4 mM NaHCO<sub>3</sub>, 0.82 mM MgSO<sub>4</sub>, 0.34 mM Ca(NO<sub>3</sub>)<sub>2</sub>, 0.41 mM CaCl<sub>2</sub>, 100 units/ml penicillin, 100  $\mu\text{g}/\text{mL}$  streptomycin) at 18 °C for 3 days before measurements. Electrophysiological experiments were performed exactly as described before (Gonzalez-Salgado et al. 2012, 2015) but comparing the effects of different concentrations of either *myo*-inositol or P<sub>i</sub>, or both.



## Statistical analysis

In all cases, at least three independent experiments were performed in triplicate. The values shown in all experiments represent the mean  $\pm$  SE. Kinetic parameters (apparent  $K_{0.5}$  and  $V_{\max}$  values) were calculated using nonlinear regression analysis of the data to the Michaelis–Menten equation. Relative expression and  $\Delta\Delta Ct$  values were calculated from the  $Ct$  (cycle threshold) values obtained from qPCR as described elsewhere (Nordgård et al. 2006). The mean  $\Delta\Delta Ct$  values obtained from our experiments were subjected to Grubb's test to detect outliers (Burns et al. 2005), and a comparison among the different conditions was made using an unpaired t-test or Student's t-test. Differences were considered significant at  $p < 0.05$ . The relative expression values ( $2^{-\Delta\Delta Ct}$ ) were used only for graphic construction. All statistical analyses were performed using Prism 5.0 software (GraphPad Software, San Diego, USA).

## Results

### Characterization and kinetic parameters of $P_i$ uptake by procyclic forms

To investigate if procyclic forms of *T. brucei* are able to take up  $P_i$ , trace amounts of  $^{32}P_i$  were added to the cell suspensions and time-dependent incorporation of label into parasites was determined by measuring the radioactivity in the cell pellet

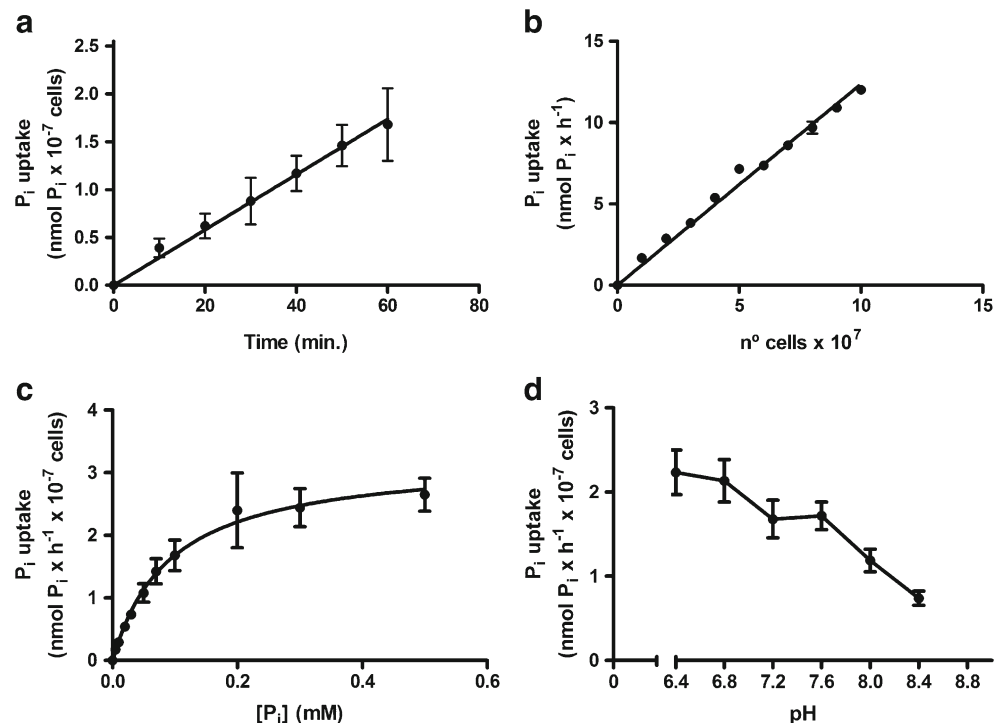
after centrifugation and disrupting the cells with SDS. As shown in Fig. 1a, procyclic forms of *T. brucei* are able to incorporate  $^{32}P_i$  and this uptake is linear for 60 min. Longer times of incorporation could possibly lead to saturation, but our aim was solely to analyze the linear phase of transport to determine the apparent kinetic parameters. In addition,  $P_i$  uptake also increased linearly with the cell number (Fig. 1b). The affinity for  $P_i$  uptake by the parasites was evaluated, revealing that  $P_i$  transport followed Michaelis–Menten kinetics over the  $P_i$  concentration range of 5–500  $\mu M$  (Fig. 1c). The transporter kinetic parameter values were calculated and revealed an apparent  $K_{0.5} = 0.093 \pm 0.008$  mM and a  $V_{\max} = 3.2 \pm 0.1$  nmol  $\times$  min $^{-1} \times 10^{-7}$  cells.

The supernatant of  $P_i$  transport medium was used to verify the presence of  $^{32}P_i$ . PEI-cellulose chromatogram was used to reveal the prominent radioactive spots and compared to the relative migration of standard [ $^{32}P_i$ ] $P_i$ . No other radiolabeled molecule was observed between the origin and [ $^{32}P_i$ ] $P_i$  (Fig. S1).

It has been reported earlier that the optimum pH for  $H^+$ -dependent  $P_i$  transport is in the acidic range, which may reflect a preference for transport of phosphate in protonated forms. pH values ranging from 6.4 to 8.4 were tested, and the transport in the acidic pH was higher than in alkaline pH, as shown in Fig. 1d. Thus, all the following experiments were performed at pH 7.2, the same as the parasite culture medium.

Maintaining nutrient homeostasis is critical to all cells and in particular to microorganisms, whose environment fluctuates in unpredictable ways. When nutrients are depleted,

**Fig. 1** Kinetic parameters of  $P_i$  transport by *T. b. brucei*: time course (a), effect of cell density (b), dependence of  $P_i$  on  $^{32}P_i$  influx (c) and effect of pH (d). Intact cells were incubated at 25 °C in a reaction mixture containing 140 mM choline chloride, 5 mM KCl, 1.5 mM  $CaCl_2$ , 10 mM HEPES (pH 7.2), 1 mM  $MgCl_2$ , 0.1 mM  $KH_2PO_4$ , 2.5  $\mu Ci/nmol$   $^{32}P_i$ , (a) either for different times with  $5 \times 10^{-7}$  cells/ml; (b) with different cell concentrations for 1 h as shown in abscissa; (c) in various concentrations of  $KH_2PO_4$  (0–0.5 mM) for 1 h or (d) with 10 mM HEPES-Mes-Tris with a pH ranging between 6.4 and 8.4. In this pH range, the cells were viable throughout the experiment. The data shown are the mean activities  $\pm$  SEM of at least three experiments, with different cell suspensions



low-affinity transporters are replaced by high-affinity ones (Levy et al. 2011). Therefore, we measured  $P_i$  transport activity in cells growing at low (1 mM) and high (10 mM) concentration of  $P_i$ . As expected, based on observations with other heteroxenic trypanosomatids (Dick et al. 2014),  $P_i$  uptake was six times higher in cells cultivated at low concentrations of  $P_i$  (Fig. 2).

To assess the effect of perturbation of the parasite plasma membrane potential gradient on  $P_i$  uptake (and possibly the  $H^+$  distribution across the membrane), parasites were incubated in the absence or presence of the  $H^+$  ionophore FCCP and the  $H^+$ -pump inhibitor bafilomycin  $A_1$ . As shown in Figure 3, depolarization of the plasma membrane with FCCP reduced  $P_i$  uptake, the opposite of what happened with bafilomycin  $A_1$ . In addition, we tested the pyrophosphate analogs and pyrophosphatase inhibitors AMDP and IDP, respectively, but observed no effect of these inhibitors on  $P_i$  transport, suggesting no involvement of  $H^+$ -pyrophosphatase coupled to this  $P_i$  transport system in *T. brucei* procyclics (Fig. 3a). Finally, we found that valinomycin, a  $K^+$  ionophore, and SCH28080, a  $H^+, K^+$ -ATPase inhibitor, were able to inhibit the  $P_i$  transport in this parasite (Fig. 3a). Taken together, these data suggest the importance of  $H^+, K^+$  gradient for  $P_i$  transport, possibly via involvement of a SCH28080 sensitive -  $H^+, K^+$ -ATPase.

### ATP levels

Recently, Dick et al. (2013) suggested that FCCP, valinomycin and SCH28080 could have metabolic effects at the mitochondrial level leading to severe ATP depletion, thus indirectly affecting the active  $P_i$  uptake. Therefore, we measured the intracellular ATP content under  $P_i$  transport conditions, in the absence or presence of SCH28080, valinomycin and FCCP, which inhibit  $P_i$  transport in procyclic forms (Fig. 3a). The results showed that only FCCP led to a decrease in cellular ATP levels (Fig. 3b).

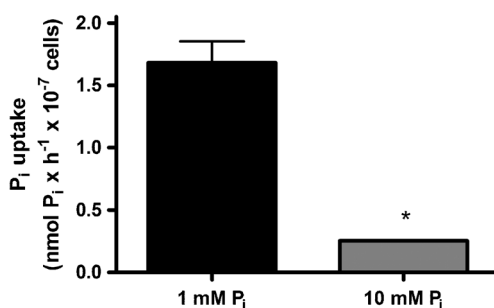


**Fig. 2** Effect of  $P_i$  concentration in the culture medium on  $P_i$  transport. Intact cells grown for 72 h in the presence of 1 or 10 mM  $P_i$  in the culture medium were incubated for 1 h at 25 °C in a reaction mixture containing 140 mM choline chloride, 5 mM KCl, 1.5 mM  $CaCl_2$ , 1 mM  $MgCl_2$ , 10 mM HEPES (pH 7.2), 0.1 mM  $KH_2PO_4$  and 2.5  $\mu Ci/nmol$   $^{32}P_i$ . The results are the means  $\pm$  S.E.M. for three independent determinations. (\*)  $p < 0.001$  by Student's *t*-test or unpaired *t*-test

### $P_i$ transport in procyclic and bloodstream forms

While *T. brucei* procyclic forms multiply in the mid-gut of the tsetse fly, bloodstream form parasites proliferate in body fluids of the mammalian host. Comparison of  $P_i$  uptake between the two life cycle forms showed that  $P_i$  transport was much higher in procyclic forms than in bloodstream forms, as measured at their respective growth temperatures, i.e. 25 °C and 37 °C, respectively (Fig. 4).

### RNA interference, growth curve, and $P_i$ transport

Using the translated protein sequence of *S. cerevisiae* Pho84 (accession number: NP\_013583.1), we identified in the TritypDB a gene encoding a protein (Tb11.02.3020) with 24% identity at the protein level to the ScPho84  $H^+ : P_i$  symporter. However, a recent study demonstrated that *Tb11.02.3020* gene encodes a *bona-fide*  $H^+$ -*myo*-inositol symporter (named TbHMIT) that is essential for normal growth of *T. brucei brucei* procyclic (Gonzalez-Salgado et al. 2012) and bloodstream forms (González-Salgado et al. 2015). In recent studies based on 3-dimensional structure of ScPho84, generated using bacterial GlpT permease as a template and multiple sequence alignments of phosphate transporters from plants, bacteria and fungi, key amino acids were identified to play an important role in phosphate transport (Ceasar et al. 2016; Samyn et al. 2012). The PSI-Coffee alignment of ScPho84 and TbHMIT (Di Tommaso et al. 2011) indicated that important functional residues in ScPho84 phosphate transporter, like the corresponding Q206, D358, Y362 and K492 residues that are important for the phosphate-binding site, and D78, R168 and E473 residues that are important for the  $H^+$ -binding site (Ceasar et al. 2016; Samyn et al. 2012), are conserved (Q177, D324, Y329 and K459, and D19, R101 and E438, respectively) in TbHMIT (data not shown). Therefore, after the biochemical characterization of the  $P_i$  transport preferences in procyclics, a cell line with TbHMIT tetracycline-inducible RNA interference (RNAi) was generated to test its potential influence in  $P_i$  transport.

For gene silencing experiments, *T. B. brucei* procyclic forms were transfected with plasmid pAG3020 (Gonzalez-Salgado et al. 2012). Initially, the plasmid pAG3020 was linearized with NotI restriction enzyme (Fig. S2A), and then was electroporated into *T. B. brucei* 29.13 procyclic forms. Parasites were then selected, and subsequently cloned by limiting dilution as described in Materials and Methods. The total DNA from several clones were isolated (data not shown) and the presence of plasmid pAG3020 in two clones were detected by PCR. As shown in Fig. S2B, amplicons were generated only in the presence of DNA isolated from parasites transfected with plasmid pAG3020 and the clone F5 was chosen for further experiments.

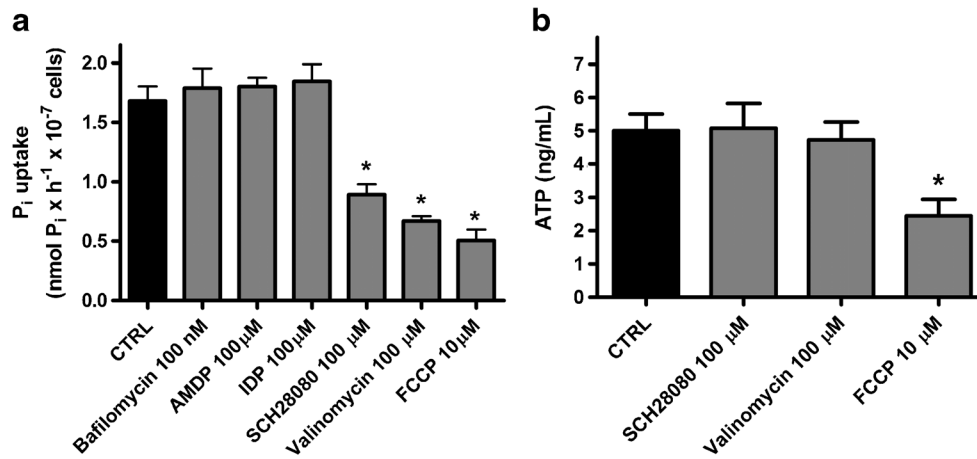


**Fig. 3** Effect of inhibitors on P<sub>i</sub> transport (a) and ATP levels (b) in *T. b. brucei*. Intact cells were incubated for 15 min at 25 °C in a reaction mixture containing 140 mM choline chloride, 5 mM KCl, 1.5 mM CaCl<sub>2</sub>, 1 mM MgCl<sub>2</sub>, 10 mM HEPES (pH 7.2), the indicated inhibitors, as shown in the abscissa; bafilomycin A<sub>1</sub> (100 nM), FCCP (10 μM), IDP (100 μM), AMDP (100 μM), valinomycin (100 μM) and SCH28080 (100 μM) and (a) 0.1 mM KH<sub>2</sub>PO<sub>4</sub>, 2.5 μCi/nmol <sup>32</sup>P<sub>i</sub> to test P<sub>i</sub>

transport or (b) 0.1 mM KH<sub>2</sub>PO<sub>4</sub> to measure the ATP levels using an ATP bioluminescent assay Kit, described in Materials and Methods. The data shown are the mean activities ± SE of at least three determinations, each with different cell suspensions. Asterisks mark significant differences (*p* < 0.05) from control, as determined by Student's *t*-test. CTRL: control of the experiment of P<sub>i</sub> transport in the presence of inhibitors vehicles (water, ethanol or dimethyl sulfoxide)

Transfected F5 cells were grown in the absence or presence of tetracycline, with the aim of inducing TbHMIT gene silencing. As expected, after the fourth day of culture, growth of cells maintained in the presence of tetracycline decreased (Fig. 5). TbHMIT mRNA levels and P<sub>i</sub> transport were compared in cells grown for two and three days in the presence of tetracycline (Fig. 6). The results show that while TbHMIT mRNA levels dropped by 80% (Fig. 6a-b), transport of P<sub>i</sub> decreased by >50% (Fig. 6c-d). Thus, in addition to impaired uptake of *myo*-inositol caused by silencing of TbHMIT (Gonzalez-Salgado et al. 2012), RNAi-induced parasites also showed reduced transport of P<sub>i</sub>. This surprising effect suggested that the transporter may

mediate both inositol and P<sub>i</sub> uptake, which prompted us to perform experiments of P<sub>i</sub> transport in the presence of increasing concentrations of *myo*-inositol. As shown in Fig. 7, there was a significant decrease in P<sub>i</sub> uptake when parasites were incubated with concentrations of *myo*-inositol higher than 300 μM.

In addition, we performed functional biochemical studies to determine if TbHMIT mediates P<sub>i</sub> transport in the *Xenopus laevis* expression system. Microinjected oocytes were perfused with different concentrations of P<sub>i</sub>. While *myo*-inositol elicited currents in these oocytes and but currents in water-injected control oocytes (Gonzalez-Salgado et al. 2012), 1 mM phosphate and 10 mM phosphate elicited similar

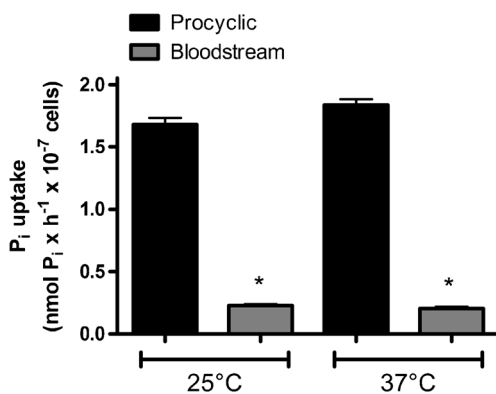


**Fig. 4** Comparison of the P<sub>i</sub> transport in bloodstream and procyclic forms of *T. b. brucei*. After obtaining the bloodstream and procyclic forms of *T. b. brucei*, the cells were incubated in buffer comprising 116 mM NaCl, 5.4 mM KCl, 55.5 mM glucose, 10 mM HEPES (pH 7.2), 0.1 mM KH<sub>2</sub>PO<sub>4</sub> and 2.5 μCi/nmol <sup>32</sup>P<sub>i</sub>. The results are the means ± S.E.M. for three independent determinations. (\*) *p* < 0.001 by Student's *t*-test

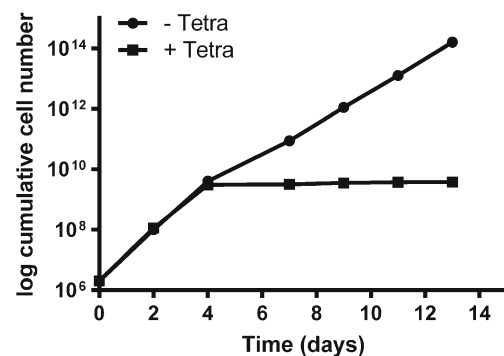


**Fig. 5** Analysis of *T. b. brucei* 29.13 + pAG30.20 growth curve in the absence or presence of tetracycline for *Tb11.02.3020* gene silencing. *Tb11.02.3020* gene was silenced and the cell growth was analyzed. Cell growth was monitored for 12 days in the absence (circles) or presence (squares) of tetracycline, using clone F5. Data shows the mean ± SEM, for at least three experiments with different cell suspensions

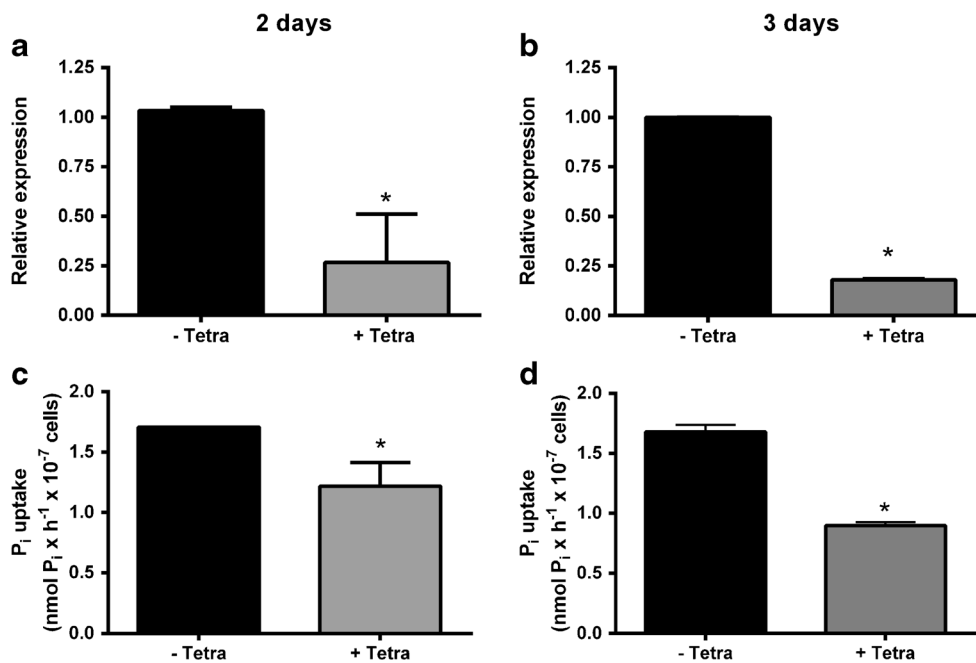


**Fig. 6** Relative expression of the *Tb11.02.3020* gene and  $P_i$  uptake in procyclic forms after induction of RNAi. Cells were grown in the absence (black bars) or presence (grey bars) of tetracyclin for 2 and 3 days, washed and used for the extraction of total RNA, which was treated with DNaseI and then used for cDNA synthesis. Differences between the cDNA level (a, b) were determined using qPCR as described in

M&M. Intact cells grown in the same conditions were incubated for 1 h at 25 °C in a reaction mixture containing 140 mM choline chloride, 5 mM KCl, 1.5 mM  $CaCl_2$ , 10 mM HEPES (pH 7.2), 1 mM  $MgCl_2$ , 2.5  $\mu Ci/nmol$   $^{32}P_i$ , and processed to compare the  $P_i$  uptake (c, d). The results are the mean  $\pm$  S.E.M. for three independent determinations. (\*)  $p < 0.001$  by Student's *t*-test or unpaired *t*-test

current amplitudes (Table 1). As expected, 100  $\mu M$  *myo*-inositol induced an ion-conductance in TbHMIT-expressing oocytes, which was not affected by 1 mM phosphate. In contrast, 10 mM phosphate significantly ( $p < 0.02$ ) decreased the current amplitude elicited by 100  $\mu M$  *myo*-inositol (Table 1). In each experiment we verified that 100  $\mu M$  *myo*-inositol elicited the same current amplitude as at the beginning of the experiment.

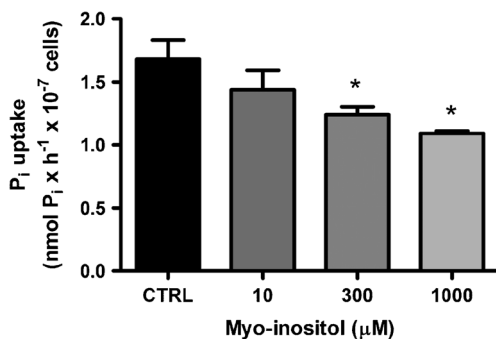


**Fig. 7** Influence of *myo*-inositol on  $P_i$  uptake in *T. b. brucei*. Intact cells were incubated for 1 h at 25 °C in a reaction mixture containing 140 mM choline chloride, 5 mM KCl, 1.5 mM  $CaCl_2$ , 10 mM HEPES (pH 7.2), 1 mM  $MgCl_2$ , 2.5  $\mu Ci/nmol$   $^{32}P_i$  in the absence or presence of *myo*-inositol (10, 300 and 1000  $\mu M$ ). The results are the mean  $\pm$  S.E.M. for three independent determinations. (\*)  $p < 0.001$  by Student's *t*-test or unpaired *t*-test. CTRL: control of  $P_i$  transport experiments (absence of *myo*-inositol)

## Discussion

$P_i$  transport in *T. b. brucei* showed a low  $K_{0.5}$  value of around 0.1 mM. In 1998, Persson et al. (1998) proposed a classification for  $P_i$  transporters in *S. cerevisiae*. According to this proposal, high-affinity  $P_i$  transport is characterized by  $K_{0.5}$  values between 0.005 and 0.015 mM, while low-affinity  $P_i$  transport is characterized by values of an apparent  $K_m$  for external phosphate of approximately 0.8 mM (Persson et al. 1998; Dick et al. 2014). It has been recently revised that other protozoan parasites, such as *T. rangeli*, *T. cruzi* and *L. infantum*, show  $K_{0.5}$  values for  $P_i$  transport of 0.045, 0.073 and 0.016 mM, respectively (Dick et al. 2014). In addition, Fig. 1d shows the optimum pH for  $P_i$  transport in the acidic pH range, confirming the literature data that there is more transport activity in acid pH, using mainly  $P_i$  as  $H_2PO_4$  form which is available in this pH range. This result has a different profile from that presented by *L. infantum*, but has similar profile to that presented by *P. falciparum* and *T. cruzi*, in which  $P_i$  uptake is via a carrier with a strong preference for  $H_2PO_4$  (Saliba et al. 2006; Russo-Abrahão et al. 2013; Dick et al. 2013). Under physiological conditions, the extracellular pH varies also with the relative proportions of monovalent ( $H_2PO_4^-$ ) and divalent ( $HPO_4^{2-}$ )  $P_i$ . At pH below 6.0,  $P_i$  is present mainly as  $H_2PO_4^-$ , whereas with increasing of pH,  $P_i$  is present as  $HPO_4^{2-}$ .



**Table 1** Current amplitudes elicited by different substrates in TbHMIT-injected and water-injected control oocytes

Injection	1 mM Phosphate	10 mM Phosphate	100 $\mu$ M <i>myo</i> -Inositol	100 $\mu$ M <i>myo</i> -Inositol + 1 mM Phosphate	100 $\mu$ M <i>myo</i> -Inositol + 10 mM Phosphate
TbHMIT ( $n = 6-9$ )	4.2 $\pm$ 0.4 nA	8.6 $\pm$ 0.9 nA	24.5 $\pm$ 0.7 nA	25.2 $\pm$ 0.4 nA	25.3 $\pm$ 1.1 nA
Water ( $n = 6-7$ )	3.8 $\pm$ 0.4 nA	6.8 $\pm$ 1.2 nA	3.0 $\pm$ 0.4 nA	4.9 $\pm$ 0.6 nA	8.2 $\pm$ 1.4 nA
Mediated by TbHMIT	0.4 $\pm$ 1.6 nA	1.8 $\pm$ 3.7 nA	21.5 $\pm$ 2.5 nA	20.3 $\pm$ 2.0 nA	16.2 $\pm$ 3.8 nA

Values are given as mean  $\pm$  SEM. Error propagation was used to determine the uncertainty of the current mediated by TbHMIT

“n” means de number of experiments performed in duplicates/triplicates

It has been reported that high affinity  $P_i$  transporters in *L. infantum* have higher mRNA levels (twice) when cells are grown at low  $P_i$  concentration (Russo-Abrahão et al. 2013). In *S. cerevisiae*, PHO84 transcript was expressed only when the cells were grown in a low  $P_i$  medium (Bun-Ya et al. 1991), suggesting that PHO84 is regulated at the transcriptional level by  $P_i$ . In *T. b. brucei*, procyclic forms grown at low concentration of  $P_i$  (1 mM) showed higher  $P_i$  transport activity than cells grown at high  $P_i$  concentration (10 mM).

In *S. cerevisiae*, the phosphate metabolism signal transduction pathway (PHO pathway) regulates the expression of several genes involved in the availability and absorption of phosphate from extracellular sources (Auesukaree et al. 2003). In environments with high  $P_i$  concentrations, a negative regulatory complex is formed between Pho80 protein (cyclin) and Pho85 protein (cyclin-dependent kinase protein, CDK), which inhibits the function of pho4 activator through its hyperphosphorylation. As the phosphorylated form of the pho4 is located predominantly in the cytoplasm, the Pho-genes transcription (*Pho5*, *Pho84* and *Pho89*) are disrupted. Under conditions of low  $P_i$  concentrations, the Pho81 protein (CDK inhibitor) inhibits the activity of Pho80-Pho85 complex, pho4 remains dephosphorylated and localized in the nucleus, where it activates Pho-genes transcription (Persson et al. 1999). A positive “feedback” mechanism has been described in PHO pathway. Phosphate limiting conditions reduce the low affinity transporter expression and thus activate the PHO pathway, including non-repression of Pho84 carrier. When the phosphate concentration increases, the proteins are also degraded and removed from the plasma membrane (Lundh et al. 2009). In a *T. brucei* BlastP analysis, we identified two protein sequences showing high similarities to *S. cerevisiae* Pho80 (accession number: AJT93899.1) and Pho85 (accession number: NP\_015294.1) proteins. It is tempting to speculate that *T. brucei* parasites sense environmental  $P_i$  in a similar way as yeast and increase  $P_i$  transport under conditions of low extracellular  $P_i$  levels.

While procyclic forms possess a cytochrome dependent mitochondrial respiratory chain and a reduced level of alternative oxidase, bloodstream forms lack cytochromes involved in the cell redox balance and cell signaling, depending only on alternative independent cytochrome oxidase and glycolysis to obtain ATP (Bakker et al. 1999; Chaudhuri et al. 2006).

Bloodstream forms do not have a functional Krebs cycle or oxidative phosphorylation, and are unable to store carbohydrates. Furthermore, glycolysis in trypanosomes and other members of the Kinetoplastida is very different of other cells and the glycosomes are the major source of ATP production in *T. brucei* bloodstream forms (Clarkson et al. 1989; Bakker et al. 1999; Chaudhuri et al. 2006; Singha et al. 2009). Because they have diverse metabolisms and inhabit different environments with challenging availabilities of  $P_i$ , we compared the  $P_i$  transport rate in these two forms of *T. brucei*.  $P_i$  transport was much higher in procyclics than in bloodstream forms, both at 25 °C and 37 °C, the optimum temperature for growth of the later forms. There may be at least two reasons for this fact: the availability of  $P_i$  is different in the insect gut and mammalian host blood, or metabolic demand for ATP production regulates how much  $P_i$  is transported into the cells. The  $P_i$  concentration was measured in the mice blood and showed a concentration of 5 mM. This concentration is higher than  $P_i$  concentration found in the SDM79 medium and the levels of  $P_i$  transport are similar to cells grown in 10 mM of  $P_i$  (data not shown). Thus, this result supports the first hypothesis suggested above. However, we cannot rule out the involvement of both hypotheses.

In 1996, Fristedt and colleagues described the importance of proton motive force generated by the activation of a  $H^+$ -ATPase, favoring the proton gradient across the plasma membrane in *S. cerevisiae* (Fristedt et al. 1996). In *T. B. brucei*, the bafilomycin  $A_1$  was not able to inhibit the transport  $P_i$ , unlike FCCP, which can lead to a dissipation of the proton gradient damaging  $P_i$  transport. In *S. cerevisiae*, the phosphate uptake activity was reduced in the presence of carbonyl cyanide m-chlorophenylhydrazone (CCCP), a chemical inhibitor of oxidative phosphorylation, demonstrating that the dissipation of the proton gradient exerts a limitation of  $Na^+$ -dependent  $P_i$  transport by Pho89 (Zvyagilskaya et al. 2008). A similar result was observed with *L. infantum* since Valinomycin, a  $K^+$  ionophore, and SCH28080,  $H^+$ , $K^+$ -ATPase inhibitor, also inhibited  $P_i$  transport (Russo-Abrahão et al. 2013). These data suggest the importance of  $H^+$  and  $K^+$  gradient to  $P_i$  transport (Villa-Bellosta and Sorribas 2010), possibly by the involvement of an SCH28080 sensitive-  $H^+$ , $K^+$ -ATPase that would sustain the protons flow, collaborating with  $P_i$  transport.

After  $P_i$  entry into cells, it may be used for energy production (ATP) in mitochondria, or stored in organelles, such as contractile vacuole complex and acidocalcisomes, acidic organelles capable of storing mainly calcium and polyphosphate (polyP) (Docampo et al. 1995; Huang et al. 2014; Jimenez and Docampo 2015). Proteomic studies recently demonstrated the presence of an orthologue of the low-affinity  $Na^+/P_i$  transporter Pho91 of *S. cerevisiae* (Tb927.11.11160) that is localized in acidocalcisomes of *T. brucei*, where it is expected to export  $P_i$  from this organelle to the cytosol (Huang et al. 2014). Two pumps are also present in these organelles: the vacuolar type  $H^+$ -ATPase (V- $H^+$ -ATPase), sensitive to bafilomycin  $A_1$ , and the vacuolar-type  $H^+$ -pyrophosphatase (V- $H^+$ -PPase), sensitive to IDP and AMDP (Vercesi et al. 1994; Rodrigues et al. 1999; Huang et al. 2014). IDP and AMDP are analogs of pyrophosphate and pyrophosphatase inhibitors, so they were tested in *T. B. brucei*  $P_i$  transport, in order to investigate the role of acidocalcisomes in  $P_i$  storage. However there is no modulation of  $P_i$  transport by these compounds, indicating no involvement of a pyrophosphatase coupled to this system, which could maintain the flow of  $H^+$  coupled to the transport of  $P_i$ .

The results obtained here using the inhibitors prompted us to investigate if these inhibitions affected the  $P_i$  carrier directly or if they had some other effect impairing the transport of  $P_i$  by the cells, such as the inhibition of ATP production. It was therefore measured the intracellular ATP content in  $P_i$  transport conditions, in the absence or presence of SCH28080, valinomycin and FCCP, inhibitors that negatively modulate  $P_i$  transport. Only FCCP led to a decrease in ATP levels, which can also be considered to be sufficient to sustain ATP-dependent  $P_i$  transport.

As mentioned above, because of similarities with the sequence of the  $H^+/P_i$  cotransporter Pho84 from *S. cerevisiae* (Ceasar et al. 2016; Persson et al. 1998, 1999; Samyn et al. 2012), it has been hypothesized that *Tb11.02.3020* may encode a  $H^+:P_i$  symporter in *T. brucei* similar to other trypanosomatids (Dick et al. 2014; Russo-Abrahão et al. 2013). The high similarity between *T. brucei* PHO84 sequence and PHO84 sequences from other Trypanosomatids was corroborated by phylogenetic trees recently published (Russo-Abrahão et al. 2013; Vieira-Bernardo et al. 2017), suggesting that these proteins have been conserved throughout trypanosomatid evolution (Russo-Abrahão et al. 2013). However, a recent study determined that *Tb11.02.3020* encodes a  $H^+$ -*myo*-inositol symporter (TbHMIT) which is mainly localized in the Golgi, is implicated in inositol-phospholipid synthesis and is essential for normal growth of *T. brucei* procyclic and bloodstream forms (Gonzalez-Salgado et al. 2012, 2015). We now found that RNAi-mediated depletion of *TbHMIT* caused not only a defect in parasite growth but also led to a 50% drop in the uptake of  $P_i$ . In addition, it

was also shown that the  $P_i$  transport was only inhibited if procyclic form parasites were placed in concentrations of *myo*-inositol higher than 300  $\mu$ M. Studies in *Xenopus* oocytes revealed that TbHMIT elicited currents after addition of *myo*-inositol (Gonzalez-Salgado et al. 2012,  $P_i$  failed to do so. However, the presence of 10 mM phosphate significantly ( $p < 0.02$ ) decreased the current amplitude elicited by 100  $\mu$ M *myo*-inositol in *Xenopus* oocytes. The electrophysiological experiments indicate that the protein encoded by *TbHMIT* is a *myo*-inositol transporter that may be only marginally affected by the presence of  $P_i$ . However, it is unclear whether phosphate is an electroneutral substrate of TbHMIT or if it competes with the binding of *myo*-inositol. Therefore, although the *TbHMIT* gene product may not transport both substrates, it seems to modulate  $P_i$  uptake in parasites in culture.

One possibility to explain the decrease of  $P_i$  transport could be related to an effect mediated by the transport of protons and *myo*-inositol that could influence the uptake of  $P_i$ . Another possibility would be the formation of a complex transport system composed by two or multiple proteins that interact at the membrane and modulate/control the uptake of common (in this case  $H^+$ ) and different compounds (such as *myo*-inositol and  $P_i$ ). So far, no other candidates were identified to fulfill these transport requirements in *T. brucei*, and additional studies involving molecular and proteomic approaches will be necessary to solve the challenging observations described here.

In conclusion, plasma membrane potential plays an important role in cell functions. In the case of most eukaryotic cells, plasma membrane potential arises primarily as a result of the passive diffusion of ions across the plasma membrane with a contribution from the electrogenic translocation of ions by ion pumps (Nolan and Voorheis 2000). It has been demonstrated that an electrogenic  $H^+$ -ATPase plays a significant role in the maintenance of the membrane potential in both bloodstream and procyclic forms of *T. brucei* (Van Der Heyden and Docampo 2002). In addition, a plasma membrane  $K^+/H^+$ -ATPase, sensitive to inhibitors of the gastric  $K^+/H^+$ -ATPase and previously identified as a  $H^+$ -ATPase, was described in *Leishmania donovani* (Jiang et al. 1994). Together with the results presented in this work showing that  $P_i$  transport is inhibited by another inhibitor of  $H^+/K^+$ -ATPase, it is possible to infer that  $H^+,K^+$ -ATPase has an important role in maintaining the flow of  $H^+$  that supports the  $P_i$  transporter in *T. brucei*.

**Acknowledgements** We would like to thank Mr. Fabiano Ferreira Esteves, Mr. Edimilson Pereira and Ms. Rosângela Rosa de Araújo for their excellent technical assistance.

**Compliance with ethical standards**

**Funding** This work was supported by grants from the Brazilian Agencies Conselho Nacional de Desenvolvimento Científico e

Tecnológico (CNPq 401134/2014–8), Coordenação de Aperfeiçoamento de Pessoal de Nível Superior (CAPES), Fundação Carlos Chagas Filho de Amparo à Pesquisa do Estado do Rio de Janeiro (FAPERJ e-26/201.300/2014) and Instituto Nacional de Ciência e Tecnologia de Biologia Estrutural e Bioimagem (INBEB). Additional funding was obtained from Swiss National Science Foundation grant CRSII3\_141913 (to E.S. and P.B.).

## References

- Auesukaree C, Homma T, Kaneko Y, Harashima S (2003) Transcriptional regulation of phosphate-responsive genes in low-affinity phosphate-transporter-defective mutants in *Saccharomyces cerevisiae*. *Biochem Biophys Res Commun* 306(4):843–850
- Bakker BM, Michels PAM, Opperdoes FR, Westerhoff HV (1999) What controls glycolysis in bloodstream form *Trypanosoma brucei*? *J Biol Chem* 274(21):14551–14559
- Beschin A, Abbeele JVD, De Baetselier P, Pays E (2014) African trypanosome control in the insect vector and mammalian host. *Trends Parasitol* 30(11):538–547
- Bun-Ya M, Nishimura M, Harashima S, Oshima Y (1991) The *Pho84* Gene or *Saccharomyces cerevisiae* encodes an inorganic phosphate transporter. *Mol Cell Biol* 11:3229–3238
- Burns MJ, Nixon GJ, Foy CA, Harris N (2005) Standardisation of data from real-time quantitative PCR methods – evaluation of outliers and comparison of calibration curves. *BMC Biotechnol* 5:31
- Cesar SA, Baker A, Muench SP, Ignacimuthu S, Baldwin SA (2016) The conservation of phosphate-binding residues among PHT1 transporters suggests that distinct transport affinities are unlikely to result from differences in the phosphate-binding site. *Biochem Soc Trans* 44:1541–1548
- Chaudhuri M, Ott RD, Hill GC (2006) Trypanosome alternative oxidase: from molecule to function. *Trends In Parasitol* 22(10):484–491
- Chintagari NR, Mishra A, Su L, Wang Y, Ayalew S, Hartson SD et al (2010) Vacuolar ATPase regulates surfactant secretion in rat alveolar type ii cells by modulating lamellar body calcium. *PLoS One* 16(5):E9228
- Clarkson AB Jr, Bienen EJ, Pollakisz G, Grady RW (1989) Respiration of bloodstream forms of the parasite *Trypanosoma brucei brucei* is dependent on a plant-like alternative oxidase. *J Biol Chem* 264(30):17770–17776
- De Koning HP, Watson CJ, Sutcliffe L, Jarvis SM (2000) Differential regulation of nucleoside and nucleobase transporters in *Crithidia fasciculata* and *Trypanosoma brucei brucei*. *Mol Biochem Parasitol* 106:93–107
- de Souza Leite M, Thomaz R, Fonseca FV, Panizzutti R, Vercesi AE, Meyer-Fernandes JR (2007) *Trypanosoma brucei brucei*: biochemical characterization of Ecto-nucleoside triphosphate Diphosphohydrolase activities. *Exp Parasitol* 115(4):315–323
- Di Tommaso P, Moretti S, Xenarios I, Orobitg M, Montanyola A, Chang JM, Taly JF, Notredame C (2011) T-coffee: a web server for the multiple sequence alignment of protein and RNA sequences using structural information and homology extension. *Nucleic Acids Res* 39:W13–W17
- Dick CF, Santos ALA, Majerowicz D, Gondim KC, Caruso-Neves C, Silva IV et al (2012) Na<sup>+</sup> –dependent and Na<sup>+</sup> –independent mechanisms for inorganic phosphate uptake in *Trypanosoma rangeli*. *Biochim Biophys Acta* 1820(7):1001–1008
- Dick CF, Santos ALA, Majerowicz D, Paes LS, Giarola NLL, Gondim KC et al (2013) Inorganic phosphate uptake in *Trypanosoma cruzi* is coupled to K<sup>(+)</sup> cycling and to active Na<sup>(+)</sup> extrusion. *Biochim Biophys Acta* 1830(8):4265–4273
- Dick CF, Santos ALA, Meyer-Fernandes JR (2014) Inorganic phosphate uptake in unicellular eukaryotes. *Biochim Biophys Acta* 1840(7):2123–2127
- Docampo R, Scott DA, Vercesi AE, Moreno SN (1995) Intracellular Ca<sup>2+</sup> storage in acidocalcisomes of *Trypanosoma cruzi*. *Biochem J* 310:1005–1012
- Food And Agriculture Organization (2015) Available: <http://www.fao.org/ag/againfo/programmes/en/paat/disease.html>, Accessed 28 September 2015
- Fristedt U, Berhe A, Ensler K, Norling B, Persson BL (1996) Isolation and characterization of membrane vesicles of *Saccharomyces cerevisiae* harboring the high-affinity phosphate transporter. *Arch Biochem Biophys* 330(1):133–141
- Giarola NL, de-Almeida-Amaral EE, Collopy-Júnior I, Fonseca-De-Souza AL, Majerowicz D, Paes LS et al (2013) *Trypanosoma cruzi*: effects of heat shock on Ecto-ATPase activity. *Exp Parasitol* 133(4):434–441
- Gonzalez-Salgado A, Steinmann ME, Greganova E, Rauch M, Mäser P, Sigel E et al (2012) *Myo*-inositol uptake is essential for bulk inositol phospholipid but not glycosylphosphatidylinositol synthesis in *Trypanosoma brucei*. *J Biol Chem* 287(16):13313–13323
- González-Salgado A, Steinmann M, Major LL, Sigel E, Reymond JL, Smith TK, Büttikofer P (2015) *Trypanosoma brucei* bloodstream forms depend upon uptake of *myo*-inositol for Golgi complex phosphatidylinositol synthesis and normal cell growth. *Eukaryot Cell* 6:616–624
- Harris RM, Webb DC, Howitt SM, Cox GB (2001) Characterization of Pita and Pitb from *Escherichia coli*. *J Bacteriol* 183(17):5008–5014
- Huang G, Ulrich PN, Storey M, Johnson D, Tischer J, Tovar JA, Moreno SN, Orlando R, Docampo R (2014) Proteomic analysis of the acidocalcisome, an organelle conserved from bacteria to human cells. *PLoS Pathog* 11 10(12):e1004555
- Ito M, Matsuka N, Izuka M, Haito S, Sakai Y et al (2005) Characterization of inorganic phosphate transport in osteoclast-like cells. *Am J Physiol Cell Physiol* 288:C921–C931
- Jiang S, Anderson SA, Winget CD, Mikkada AJ (1994) Plasma Membrane K<sup>+</sup>/H<sup>+</sup> + –ATPase From *Leishmania donovani*. *J Cell Physiol* 159:60–66
- Jimenez V, Docampo R (2015) TcPho91 is a contractile vacuole phosphate sodium symporter that regulates phosphate and polyphosphate metabolism in *Trypanosoma cruzi*. *Mol Microbiol* 97(5):911–925
- Kriel J, Haesendonckx S, Rubio-Teixeira M, Zeebroeck GV, Thevelein JM (2011) From transporter to transceptor: signaling from transporters provokes Re-evaluation of complex trafficking and regulatory controls. *Bioassays* 33:870–879
- Lamarque MG, Wanner BL, Crépin S, Harel J (2008) The phosphate regulon and bacterial virulence: a regulatory network connecting phosphate homeostasis and pathogenesis. *FEMS Microbiol Rev* 32(3):461–473
- Levy S, Kafri M, Carmi M, Barkai N (2011) The competitive advantage of a dual-transporter system. *Science* 334:1408–1412
- Lopes AH, Souto-Padrón T, Dias FA, Gomes MT, Rodrigues GC, Zimmermann LT et al (2010) Trypanosomatids: Odd Organisms. *Devastating Diseases, Open Parasitol J* 4:30–59
- Lundh F, Mouillon J, Samyn D, Stadler K, Popova Y, Lagerstedt JO, Thevelein JM, Persson BL (2009) Molecular mechanisms controlling phosphate-induced downregulation of the yeast Pho84 phosphate transporter. *Biochemistry* 48:4497–4505
- Marchesini N, Docampo R (2002) A plasma membrane P-type H<sup>(+)</sup>-ATPase regulates intracellular pH in *Leishmania mexicana amazonensis*. *Mol Biochem Parasitol* 119(2):225–236
- Martinez P, Persson BL (1998) Identification, cloning and characterization of a Derepressible Na<sup>+</sup> –coupled phosphate transporter in *Saccharomyces cerevisiae*. *Mol Gen Genet* 258(6):628–638

- Martinez R, Wang Y, Benaim G, Benchimol M, De-Souza W, Scott D et al (2002) A proton pumping pyrophosphatase in the Golgi apparatus and plasma membrane vesicles of *Trypanosoma cruzi*. *Mol Biochem Parasitol* 120:205–213
- Martins RM, Covarrubias C, Rojas RG, Silber AM, Yoshida N (2009) Use of L-proline and ATP production by *Trypanosoma cruzi* Metacyclic forms as requirements for host cell invasions. *Infect Immun* 77:3023–3032
- Mosmann T (1983) Rapid colorimetric assay for cellular growth and survival: application to proliferation and cytotoxicity assays. *J Immunol Methods* 65:55–63
- Nolan DP, Voorheis HP (2000) Factors that determine the plasma-membrane potential in bloodstream forms of *Trypanosoma brucei*. *Eur J Biochem* 267:4615–4623
- Nordgård O, Kvaløy JT, Farmen RK, Heikkilä R (2006) Error propagation in relative real-time reverse transcription polymerase chain reaction quantification models: the balance between accuracy and precision. *Anal Biochem* 356:182–193
- Pavón LR, Lundh F, Lundin B, Mishra A, Persson BL, Spetea C (2008) *Arabidopsis* Antr1 is a thylakoid Na<sup>+</sup>-dependent phosphate transporter. *J Biol Chem* 283(20):13520–13527
- Persson BL, Berhe A, Fristedt U, Martinez P, Pattison J, Petersson J et al (1998) Phosphate permeases of *Saccharomyces cerevisiae*. *Biochim Biophys Acta* 1365(1–2):23–30
- Persson BL, Petersson J, Fristedt U, Weinander R, Berhe A, Pattison J (1999) Phosphate permeases of *Saccharomyces cerevisiae*: structure, function and regulation. *Biochim Biophys Acta* 16 1422(3): 255–272
- Persson BL, Lagerstedt JO, Pratt JR, Pattison-Granberg J, Lundh K, Shokrollahzadeh D et al (2003) Regulation of phosphate acquisition in *Saccharomyces cerevisiae*. *Curr Genet* 43(4):225–244
- Rodrigues CO, Scott DA, Docampo R (1999) Characterization of a vacuolar pyrophosphatase in *Trypanosoma brucei* and its localization to acidocalcisomes. *Mol Cell Biol* 19(11):7712–7723
- Rozen S, Skaletsky HJ (2000) Primer3 on the WWW for general users and for biologist programmers. In: S. Krawetz, S. Misener. (Eds.) bioinformatics methods and protocols. *Methods Mol Biol* 132:365–386
- Russo-Abrahão T, Alves-Bezerra M, Majerowicz D, Freitas-Mesquita AL, Dick CF, Gondim KC, Meyer-Fernandes JR (2013) Transport of inorganic phosphate in *Leishmania infantum* and compensatory regulation at low inorganic phosphate concentration. *Biochim Biophys Acta* 1830(3):2683–2689
- Saliba KJ, Martin RE, Bröer A, Henry RI, McCarthy CS et al (2006) Sodium-dependent uptake of inorganic phosphate by the intracellular malaria parasite. *Nature* 443:582–585
- Samyn DR, Ruiz-Pavon L, Andersson MR, Popova Y, Thevelein JM, Persson BL (2012) Mutational analysis of putative phosphate- and proton-binding sites in the *Saccharomyces cerevisiae* Pho84 phosphate:H<sup>+</sup> transceptor and its effect on Signalling to the PKA and PHO pathways. *Biochem J* 445:413–422
- Schothorst J, Kankipati HN, Conrad M, Samyn DR, Zeebroeck GV, Popova Y et al (2013) Yeast nutrient Transceptors provide novel insight in the functionality of membrane transporters. *Curr Genet* 59:197–206
- Singha UK, Sharma S, Chaudhuri M (2009) Downregulation of mitochondrial Porin inhibits cell growth and alters respiratory phenotype in *Trypanosoma brucei*. *Eukaryot Cell* 8(9):1418–1428
- Steverding D (2008) The history of African trypanosomiasis. *Parasit Vectors* 1(1):3
- Uyemura SA, Luo S, Vieira M, Moreno SN, Docampo R (2004) Oxidative phosphorylation and rotenone-insensitive malate- and NADH-Quinone oxidoreductases in *Plasmodium yoelii yoelii* mitochondria in situ. *J Biol Chem* 279:385–393
- Van Der Heyden N, Docampo R (2002) Significant differences between procyclic and bloodstream forms of *Trypanosoma brucei* in the maintenance of their plasma membrane potential. *J Eukaryot Microbiol* 49(5):407–413
- Vercesi AE, Moreno SN, Docampo R (1994) Ca<sup>2+</sup>/H<sup>+</sup> exchange in acidic vacuoles of *Trypanosoma brucei*. *Biochem J* 304(Pt1):227–233
- Vieira DP, Paletta-da-Silva R, Saraiva EM, Lopes AH, Meyer-Fernandes JR (2011) *Leishmania chagasi*: an Ecto-3'-Nucleotidase activity modulated by inorganic phosphate and its possible involvement in parasite-macrophage interaction. *Exp Parasitol* 127(3):702–707
- Vieira-Bernardo R, Gomes-Vieira AL, Carvalho-Kelly LF, Russo-Abrahão T, Meyer-Fernandes JR (2017) The biochemical characterization of two phosphate transport systems in *Phytomonas serpens*. *Exp Parasitol* 173:1–8
- Vieyra A, Meyer-Fernandes JR, Gama OBH (1985) Phosphorolysis of acetyl phosphate by orthophosphate with energy conservation in the Phosphoanhydride linkage of pyrophosphate. *Arch Biochem Biophys* 238(2):574–583
- Villa-Belosta R, Sorribas V (2010) Compensatory regulation of the sodium/phosphate cotransporters Napi-Iic (Scl34a3) and pit-2 (Slc20a2) during pi deprivation and acidosis. *Pflugers Arch* 459(3):499–508
- World Health Organization (2014) Available: <http://www.who.int/en/>, Accessed 20 December 2014.
- Zvyagilskaya RA, Lundh F, Samyn D, Pattison-Granberg J, Mouillon JM, Popova Y et al (2008) Characterization of the Pho89 phosphate transporter by functional Hyperexpression in *Saccharomyces cerevisiae*. *FEMS Yeast Res* 8(5):685–696